VIP Oxide–Hydrides Very Important Paper

DOI: 10.1002/ange.201403536

Strontium Vanadium Oxide–Hydrides: "Square-Planar" Two-Electron Phases**

*Fabio Denis Romero, Alice Leach, Johannes S. Möller, Francesca Foronda, Stephen J. Blundell, and Michael A. Hayward**

Abstract: *A series of strontium vanadium oxide–hydride phases prepared by utilizing a low-temperature synthesis strategy in which oxide ions in $Sr_{n+1}V_nO_{3n+1}$ ($n=\infty$, 1, 2) phases are topochemically replaced by hydride ions to form $SrVO_2H$, Sr_2VO_3H, and $Sr_3V_2O_5H_2$, respectively. These new phases contain sheets or chains of apex-linked $V^{3+}O_4$ squares stacked with SrH layers/chains, such that the $n=\infty$ member, $SrVO_2H$, can be considered to be analogous to "infinite-layer" phases, such as $Sr_{1-x}Ca_xCuO_2$ (the parent phase of the high-T_c cuprate superconductors), but with a d^2 electron count. All three oxide–hydride phases exhibit strong antiferromagnetic coupling, with $SrVO_2H$ exhibiting an antiferromagnetic ordering temperature, $T_N > 300$ K. The strong antiferromagnetic couplings are surprising given they appear to arise from π-type magnetic exchange.*

Low-temperature topochemical synthesis routes offer an alternative strategy for preparing phases containing square-planar transition-metal centers. For example, the low-temperature reductive deintercalation of oxide ions from the perovskite phases $LaNiO_3$ and $SrFeO_{3-\delta}$, using the hydride reducing agents NaH and CaH_2 respectively, yield $LaNiO_2$ and $SrFeO_2$.[1] These reduced oxides consist of infinite sheets of square-planar $Ni^{1+}O_4$ or $Fe^{2+}O_4$ centers stacked with La^{3+} or Sr^{2+} cations, respectively. By applying this reductive deintercalation approach to other perovskite oxides the catalogue of transition-metal cations that can be located in planar sites can be extended to include Co^+ ($LaBaCo_2O_{4.25}$) and Ru^{2+} ($SrFe_{0.5}Ru_{0.5}O_2$).[2] Furthermore, by utilizing layered $A_{n+1}B_nO_{3n+1}$ Ruddlesden–Popper oxides or $A_3B_2O_5Cl_2$ oxychlorides, additional lower dimensional structures containing isolated double sheets ($Sr_3M_2O_4Cl_2$, M = Fe, Co), chains ($LaSrNiO_{3+x}$, Sr_2FeO_3), or double chains ($Sr_3Fe_2O_5$) of apex-linked MO_4 squares can be prepared.[3]

Despite the growing diversity of materials containing square-planar transition metal centers, a common feature of all of these phases is a relatively high d-electron count: d^6 (Fe^{2+}, Ru^{2+}), d^7 (Co^{2+}), d^8 (Co^{1+}, Ni^{2+}, Cu^{3+}), or d^9 (Ni^{1+}, Cu^{2+}). As a consequence, most of the phases prepared are Mott–Hubbard insulators, with a strong tendency for antiferromagnetic order owing to the occupation of σ-symmetry metal d-orbitals. To extend the study of square-planar-coordinated transition-metal systems to earlier, electron-poor transition metals, we have focused on the topochemical reduction of V^{4+} oxides.

The reaction of the perovskite phase $SrVO_3$ with CaH_2 at 610 °C results in the formation of a new tetragonal phase (*P4/mmm*: $a = 3.93$ Å, $c = 3.66$ Å). X-ray powder diffraction data show that the cation lattice of $SrVO_3$ is retained in the new material; however, neutron powder diffraction data (Supporting Information, Figure S1) and chemical titrations indicate that rather than a simple oxygen deintercalation process to form $SrVO_{3-x}$ (as has been previously observed for a wide variety of other transition metal perovskite oxides[4]), reaction with CaH_2 results in an anion exchange reaction and the formation of the oxide–hydride phase $SrVO_2H$ (Figure 1 a), with CaO being the other solid product (full details of the structural refinement strategy are given in the Supporting Information).

The anion exchange of oxide for hydride in an extended solid is rare but not unprecedented. Analogous reactions have

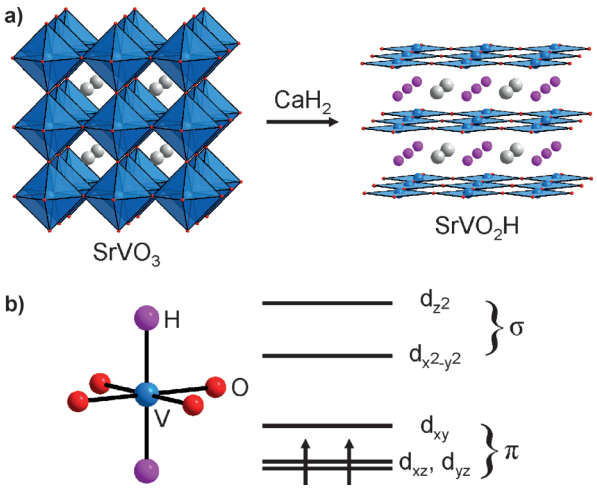

Figure 1. Crystal and local electronic structure of $SrVO_2H$. a) The cubic perovskite $SrVO_3$ is transformed topochemically into the tetragonal oxide–hydride $SrVO_2H$ by the action of CaH_2 at 610 °C. Sr gray, V blue, O red, H pink. b) The local O_4H_2 coordination of vanadium results in a $(d_{xy}, d_{xz})^2$ electronic state.

[*] Dr. F. Denis Romero, A. Leach, Prof. M. A. Hayward
Department of Chemistry, Inorganic Chemistry Laboratory
University of Oxford, South Parks Road, Oxford, OX1 3QR (UK)
E-mail: michael.hayward@chem.ox.ac.uk
Dr. J. S. Möller, F. Foronda, Prof. S. J. Blundell
Department of Physics, Clarendon Laboratory
University of Oxford, Parks Road, Oxford, OX1 3PU (UK)

[**] We thank R. Smith for assistance collecting the neutron powder diffraction data. Experiments at the ISIS pulsed neutron facility were supported by a beam time allocation from the STFC. Part of this work was performed at the Swiss Muon Source, and we thank H. Luetkensfor technical assistance and the EPSRC for financial support.

Supporting information for this article is available on the WWW under http://dx.doi.org/10.1002/anie.201403536.

 © 2014 Wiley-VCH Verlag GmbH & Co. KGaA, Weinheim

been observed when the cobalt Ruddlesden–Popper phases $LaSrCoO_4$ and $Sr_3Co_2O_{7-x}$ react with CaH_2 to form $LaSrCoO_3H_{0.7}$ and $Sr_3Co_2O_{4.33}H_{0.84}$ respectively, and when $ATiO_3$ (A = Ba, Sr, Ca) phases react with CaH_2 to form $ATiO_{3-x}H_y$.[5] What is different in this case, and previously unobserved, is that the anion-exchange reaction is stoichiometric (within the sensitivity of our measurements) and results in a fully anion-ordered phase. A direct 1:1 replacement of oxide with hydride converts $SrVO_3$ into $SrVO_2H$, accompanied by a concomitant reduction of V^{4+} to V^{3+}. It should be noted that samples contained small quantities of $SrVO_{3-x}$ owing to the presence of some $Sr_{1-\delta}VO_3$ in the starting material, as discussed in detail in the Supporting Information.

The structure of $SrVO_2H$ consists of V^{3+} cations located within square planes of oxide ions, as shown in Figure 1a. These $V^{3+}O_4$ units share corners to form infinite VO_2 sheets directly analogous the CuO_2 planes observed in $Sr_{1-x}Ca_xCuO_2$, the parent phase of the high-T_c superconducting cuprates.[6] However, unlike $Sr_{1-x}Ca_xCuO_2$ or other infinite layer phases such as $LaNiO_2$ or $SrFeO_2$, the VO_2 sheets in $SrVO_2H$ are connected by the hydride ions, which occupy the remaining two coordination sites around each V^{3+} center. Thus the structure of $SrVO_2H$ can be described by a VO_2-SrH-VO_2-SrH stacking sequence.

Despite the formal six-fold VO_4H_2 coordination of the vanadium centers in $SrVO_2H$, there is a direct structural and electronic analogy between this phase and the infinite-layer ABO_2 phases. This is because the 1s valence orbitals of the hydride ions have strict σ-type symmetry with respect to the vanadium cations and are thus orthogonal to the π symmetry d_{xz}, d_{yz}, and d_{xy} orbitals from which the HOMO (a degenerate $(d_{xz},d_{yz})^2$ pair) and LUMO (the d_{xy} orbital) of the local VO_4H_2 unit are derived (after interaction with π-type symmetry oxygen 2p orbitals), as shown in Figure 1b. Thus to a first approximation the d-electrons in $SrVO_2H$ only "see" the infinite layer V–O framework, as the σ-type vanadium d-orbitals which do interact with the H 1s orbitals are empty and energetically remote from the filled orbitals. As a result, $SrVO_2H$ can be considered directly analogous to a d^2 infinite-layer system, such as the hypothetical phase "KVO_2" in which the SrH layers are replaced by layers of potassium cations.

Analogous reactions between CaH_2 and the $n = 1$ and $n = 2$ members of the $Sr_{n+1}V_nO_{3n+1}$ Ruddlesden–Popper series also result in anion exchange reactions. Thus tetragonal Sr_2VO_4 and $Sr_3V_2O_7$ yield orthorhombic Sr_2VO_3H (*Immm*: $a = 3.88$ Å, $b = 3.66$ Å, $c = 12.77$ Å) and $Sr_3V_2O_5H_2$ (*Immm*: $a = 3.91$ Å, $b = 3.66$ Å $c = 20.63$ Å) respectively as shown in Figure 2. Full details of the structural and chemical characterization of the $Sr_{n+1}V_nO_{2n+1}H_n$ ($n = 1$, 2) phases are given in Supporting Information, Figures S2 and S3. As shown in Figure 2, Sr_2VO_3H and $Sr_3V_2O_5H_2$ are also constructed from VO_4H_2 units. However, due to the layered nature of the of the Ruddlesden–Popper "parent" phases, Sr_2VO_3H and $Sr_3V_2O_5H_2$ adopt structures containing chains or double chains of apex-linked VO_4 squares. As the local geometry at vanadium is the same in Sr_2VO_3H and $Sr_3V_2O_5H_2$ as in $SrVO_2H$, by the electronic arguments described above, these materials can be seen as the d^2 analogues of orthorhombic Sr_2CuO_3/Sr_2FeO_3 and $Sr_3Fe_2O_5$, respectively.[3d,e,7]

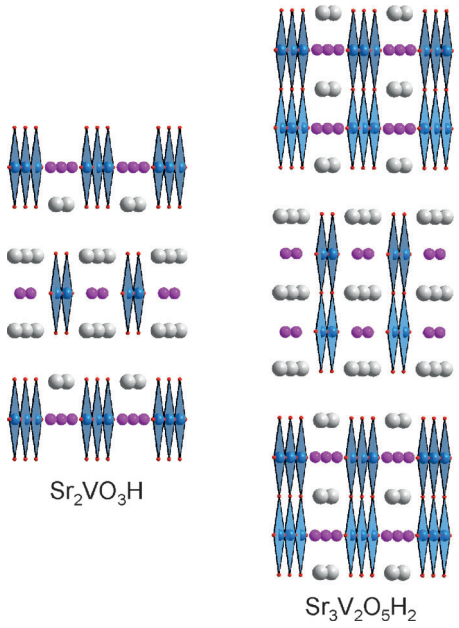

Figure 2. Reaction of Sr_2VO_4 and $Sr_3V_2O_7$ with CaH_2, resulting in the formation of the oxide–hydrides Sr_2VO_3H and $Sr_3V_2O_5H_2$, respectively. Sr gray, V blue, O red, H pink.

Examining the structures of the three $Sr_{n+1}V_nO_{2n+1}H_n$ phases reveals that the vanadium hydride bond lengths are almost identical in all three materials (V–H = 1.834(1) Å, 1.833(1) Å, and 1.834(1) Å for $n = 1$, 2, and ∞, respectively). These values compare well with bridging V–H bonds observed in silylamino(disilylamido) V^{3+} complexes, such as $[\{V(N\{N''\}_2)\}_2(\mu\text{-}H)_2]$ (V–H = 1.83(3) Å and 1.85(3) Å)[8] and the metal hydride "VH_{2-x}" (V–H = 1.84 Å)[9] and fall into the range of Co–H bond lengths observed in cobalt oxide hydride phases.[5a,b]

Neutron powder diffraction data collected at 5 K (Supporting Information, Figures S1–S3) indicate that all three oxide–hydride phases adopt the antiferromagnetically ordered states shown in Figure 3, and this behavior is confirmed by the observation of large static magnetic fields within the materials by zero-field muon-spin relaxation (μ^+SR) measurements (Supporting Information, Figure S6). On warming Sr_2VO_3H from 5 K, the ordered magnetic moment observed by neutron powder diffraction, and the static magnetic field observed by μ^+SR, decline to zero (Figure 4), consistent with an antiferromagnetic ordering temperature of $T_N \approx 170$ K. Analogous behavior is observed for $Sr_3V_2O_5H_2$ (Supporting Information, Figure S4), indicating an ordering temperature of $T_N \approx 240$ K for this phase. Rather surprisingly, neither zero-field cooled nor field cooled magnetization data collected from either Sr_2VO_3H or $Sr_3V_2O_5H_2$ show anomalies at these magnetic ordering temperatures (Figure 4; Supporting Information, Figure S4). Neutron diffraction data collected from $SrVO_2H$ at 298 K indicate that antiferromagnetic order persists to room temperature (Supporting Information, Figure S1). The ordered moments at 5 K and 298 K are rather similar (5 K: 1.56(2) μ_B; 298 K: 1.49(1) μ_B), suggesting that the antiferromagnetic ordering temperature, T_N, is much greater than 300 K.

 © 2014 Wiley-VCH Verlag GmbH & Co. KGaA, Weinheim

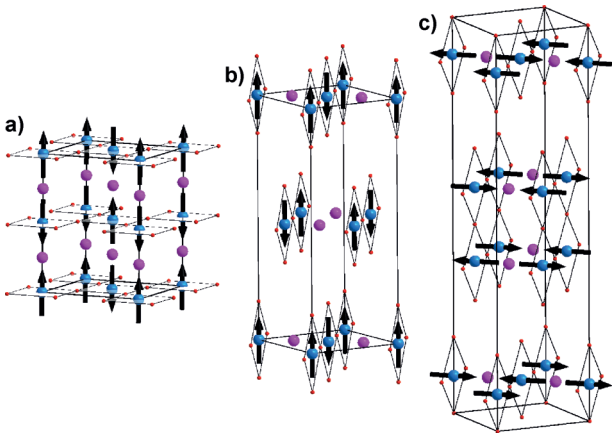

Figure 3. Refinement against neutron powder diffraction data collected at 5 K, revealing: a) $SrVO_2H$ b) Sr_2VO_3H and c) $Sr_3V_2O_5H_2$ adopt antiferromagnetically ordered states with ordered moments of 1.56(2), 1.54(5), and 1.35(8) μ_B per vanadium center, respectively. V blue, O red, H pink.

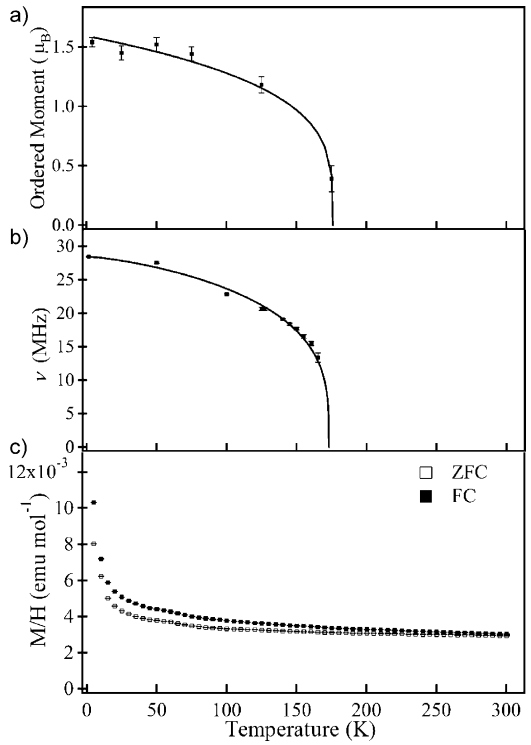

Figure 4. Magnetic data from Sr_2VO_3H. a) The ordered moment refined from neutron diffraction data, and b) the muon oscillation frequency plotted against temperature, indicating an antiferromagnetic ordering temperature of $T_N \approx 171(1)$ K. In contrast, c) the zero-field cooled and field cooled susceptibility data measured in a field of 100 Oe show no feature at this temperature.

The antiferromagnetic ordering temperatures of the $Sr_{n+1}V_nO_{2n+1}H_n$ phases reflect the decreasing dimensionality of the vanadium-anion lattices. Similar effects are observed for the structurally analogous $Sr_{n+1}Fe_nO_{2n+1}$ Fe^{2+} oxide phases: "three-dimensional" $SrVO_2H$ ($T_N > 300$ K) and $SrFeO_2$ ($T_N = 468$ K) have higher ordering temperatures than the "1.5-dimensional" $Sr_3V_2O_5H_2$ ($T_N = 240$ K), and $Sr_3Fe_2O_5$ ($T_N = 378$ K) than the "quasi one-dimensional" Sr_2VO_3H ($T_N = 170$ K) and Sr_2FeO_3 ($T_N = 179$ K).[1b,3d,e] This variation in magnetic ordering temperature with dimensionality suggests that the strengths of the magnetic couplings within the "perovskite blocks" of all three $Sr_{n+1}V_nO_{2n+1}H_n$ phases are comparable, with the variation in T_N being attributable to the presence of SrO rock salt layers in the $n = 1$ and $n = 2$ materials. The high magnetic ordering temperatures observed for $Sr_{n+1}V_nO_{2n+1}H_n$ phases are surprising given that the magnetically ordered states appear to arise exclusively from interactions between electrons in π-symmetry d-orbitals (d_{xz} and d_{yz}) rather than the much stronger σ-type superexchange between $d_{x^2-y^2}$ orbitals observed for the $Sr_{n+1}Fe_nO_{2n+1}$ series.[10]

An additional unexpected feature of the magnetic behavior of $Sr_{n+1}V_nO_{2n+1}H_n$ phases is the lack of any signature in the magnetization data at the antiferromagnetic ordering temperatures of these materials. Powder neutron diffraction data and μ^+SR data agree on the simultaneous disappearance of a long-range antiferromagnetically ordered lattice and a static magnetic field in Sr_2VO_3H at $T_N = 170$ K (Figure 4), but this event leads to no observable change in the magnetization of the material. These observations may suggest that strong dynamic magnetic correlations in Sr_2VO_3H build up well above T_N so that the entropy released at the magnetic transition is suppressed, leading to minimal change in the measured susceptibility. The sudden onset of static long-range order is nevertheless clearly manifested in the diffraction and μ^+SR data. Analogous behavior also appears to be exhibited by $Sr_3V_2O_5H_2$ (Supporting Information, Figure S4). Such unusual magnetic behavior in a chemically unique set of materials clearly warrants further investigation. Furthermore, we note that the "parent" materials of a number of unconventional superconducting phases are antiferromagnetic insulators in their undoped forms, and the unusual magnetic behavior of $Sr_{n+1}V_nO_{2n+1}H_n$ phases may be a prelude to similar behavior. Thus the $Sr_{n+1}V_nO_{2n+1}H_n$ phases reported herein do not just extended the catalogue of complex oxides containing square-planar-coordinated transition-metal centers, but offer a new low electron-count regime in which to investigate the interactions between strongly interacting transition metal d-electrons.

Experimental Section

$Sr_{n+1}V_nO_{3n+1}$ ($n = 1, 2, \infty$) phases were prepared by reduction of V^{5+} precursors under flowing hydrogen, as described previously.[11] Reduction of the $Sr_{n+1}V_nO_{3n+1}$ materials was achieved using CaH_2.[5a] Full details of the synthesis of $Sr_{n+1}V_nO_{3n+1}$ ($n = 1, 2, \infty$) phases and their subsequent conversion into $Sr_{n+1}V_nO_{2n+1}H_n$ ($n = 1, 2, \infty$) phases is given in the Supporting Information. Neutron powder diffraction data were collected using the POLARIS diffractometer (ISIS neutron source, UK) from samples contained within vanadium cans sealed under an argon atmosphere with an indium washer. Rietveld profile refinement was performed using the GSAS suite of programs.[12] Oxidative titrations were performed to determine the vanadium oxidation states of materials by dissolving samples in a 1:1 solution of sulfuric acid, followed by titration with $KMnO_4$ under inert argon atmosphere. Magnetization data were collected using

© 2014 Wiley-VCH Verlag GmbH & Co. KGaA, Weinheim

a Quantum Design MPMS SQUID magnetometer. The μ^+SR experiments were carried out at the Swiss Muon Source, PSI, Switzerland. In a μ^+SR experiment, spin-polarized muons were implanted in the bulk of a material and the time dependence of their polarization monitored by recording the angular distribution of the subsequent positron decay. All of the samples were analyzed by X-ray powder diffraction and oxidative TGA/titration to ensure they had not decomposed (oxidized) during the physical measurements.

Received: March 20, 2014
Revised: May 18, 2014
Published online: June 24, 2014

Keywords: oxide–hydrides · solid-state reactions · solid-state structures · topochemistry

[1] a) M. A. Hayward, M. A. Green, M. J. Rosseinsky, J. Sloan, *J. Am. Chem. Soc.* **1999**, *121*, 8843; b) Y. Tsujimoto, C. Tassel, N. Hayashi, T. Watanabe, H. Kageyama, K. Yoshimura, M. Takano, M. Ceretti, C. Ritter, W. Paulus, *Nature* **2007**, *450*, 1062.

[2] a) J. Seddon, E. Suard, M. A. Hayward, *J. Am. Chem. Soc.* **2010**, *132*, 2802; b) F. Denis Romero, S. J. Burr, J. E. McGrady, D. Gianolio, G. Cibin, M. A. Hayward, *J. Am. Chem. Soc.* **2013**, *135*, 1838.

[3] a) E. Dixon, M. A. Hayward, *Inorg. Chem.* **2010**, *49*, 9649; b) F. Denis Romero, L. Coyle, M. A. Hayward, *J. Am. Chem. Soc.* **2012**, *134*, 15946; c) M. Crespin, C. Landron, P. Odier, J. M. Bassat, P. Mouron, J. Choisnet, *J. Solid State Chem.* **1992**, *100*, 281; d) C. Tassel, L. Seinberg, N. Hayashi, S. Ganesanpotti, Y. Ajiro, Y. Kobayashi, H. Kageyama, *Inorg. Chem.* **2013**, *52*, 6096; e) H. Kageyama, T. Watanabe, Y. Tsujimoto, A. Kitada, Y. Sumida, K. Kanamori, K. Yoshimura, N. Hayashi, S. Muranaka, M. Takano, M. Ceretti, W. Paulus, C. Ritter, G. Andre, *Angew. Chem.* **2008**, *120*, 5824; *Angew. Chem. Int. Ed.* **2008**, *47*, 5740.

[4] a) M. A. Hayward in *Comprehensive Inorganic Chemistry II*, *Vol. 2* (Eds.: J. Reedijk, K. R. Poeppelmeier), Elsevier, Oxford, **2013**, pp. 417; b) T. Yamamoto, H. Kageyama, *Chem. Lett.* **2013**, *42*, 946.

[5] a) M. A. Hayward, E. J. Cussen, J. B. Claridge, M. Bieringer, M. J. Rosseinsky, C. J. Kiely, S. J. Blundell, I. M. Marshall, F. L. Pratt, *Science* **2002**, *295*, 1882; b) R. M. Helps, N. H. Rees, M. A. Hayward, *Inorg. Chem.* **2010**, *49*, 11062; c) Y. Kobayashi, O. J. Hernandez, T. Sakaguchi, T. Yajima, T. Roisnel, Y. Tsujimoto, M. Morita, Y. Noda, Y. Mogami, A. Kitada, M. Ohkura, S. Hosokawa, Z. F. Li, K. Hayashi, Y. Kusano, J. E. Kim, N. Tsuji, A. Fujiwara, Y. Matsushita, K. Yoshimura, K. Takegoshi, M. Inoue, M. Takano, H. Kageyama, *Nat. Mater.* **2012**, *11*, 507; d) T. Sakaguchi, Y. Kobayashi, T. Yajima, M. Ohkura, C. Tassel, F. Takeiri, S. Mitsuoka, H. Ohkubo, T. Yamamoto, J. E. Kim, N. Tsuji, A. Fujihara, Y. Matsushita, J. Hester, M. Avdeev, K. Ohoyama, H. Kageyama, *Inorg. Chem.* **2012**, *51*, 11371.

[6] a) T. Siegrist, S. M. Zahurak, D. W. Murphy, R. S. Roth, *Nature* **1988**, *334*, 231; b) M. Takano, Y. Takeda, H. Okada, M. Miyamoto, T. Kusaka, *Physica C* **1989**, *159*, 375.

[7] C. L. Teske, H. Mullerbu, *Z. Anorg. Allg. Chem.* **1969**, *371*, 325.

[8] G. P. Clancy, H. C. S. Clark, G. K. B. Clentsmith, F. G. N. Cloke, P. B. Hitchcock, *J. Chem. Soc. Dalton Trans.* **1999**, 3345.

[9] A. J. Maeland, T. R. P. Gibb, D. P. Schumacher, *J. Am. Chem. Soc.* **1961**, *83*, 3728.

[10] a) H. J. Xiang, S.-H. Wei, M. H. Whangbo, *Phys. Rev. Lett.* **2008**, *100*, 167207; b) J. M. Pruneda, J. Iniguez, E. Canadell, H. Kageyama, M. Takano, *Phys. Rev. B* **2008**, *78*, 115101; c) H. J. Koo, H. J. Xiang, C. Lee, M. H. Whangbo, *Inorg. Chem.* **2009**, *48*, 9051.

[11] M. J. Rey, P. Dehaudt, J. C. Joubert, B. Lambert Andron, M. Cyrot, F. Cyrot-Lackmann, *J. Solid State Chem.* **1990**, *86*, 101.

[12] A. C. Larson, R. B. Von Dreele, Los Alamos National Laboratory Report LAUR 86–748, **2000**.

 © 2014 Wiley-VCH Verlag GmbH & Co. KGaA, Weinheim